Int. J. Heat Mass Transfer. Vol. 19, pp. 395–403. Pergamon Press 1975. Printed in Great Britain

UNSTEADY HEAT TRANSFER IN IMPULSIVE FALKNER–SKAN FLOWS

CHARLES B. WATKINS, JR.
Department of Mechanical Engineering, Howard University, Washington, DC 20059, U.S.A.

(*Received* 28 *February* 1975 *and in revised form* 28 *May* 1975)

Abstract—Numerical solutions for heat transfer in the unsteady laminar boundary layer resulting from incompressible flow past an impulsively-started semi-infinite wedge are described. The motion of the wedge is steady after the impulsive start. A forced-convection thermal boundary layer is produced by the sudden imposition of a constant temperature difference between the wedge and the fluid as the motion is started. Solutions for the simultaneous development of the thermal and momentum boundary layers are obtained by a time-asymptotic finite-difference procedure. Results of calculations are presented for several wedge angles with Prandtl numbers in the intermediate range.

NOMENCLATURE

b, constant, see equation (18);
c_p, fluid specific heat at constant pressure;
f_x, $= \dfrac{2\sigma_s}{\rho U^2}$, local friction coefficient;
h_x, local heat-transfer coefficient;
k, fluid thermal conductivity;
L, reference length;
n, exponent in inviscid velocity relation, see equation (1);
Nu_x, $= \dfrac{h_x x^*}{k}$, local Nusselt number;
Pr, $= \dfrac{c_p \mu}{k}$, Prandtl number;
Re_x, $= \dfrac{x^* U \rho}{\mu}$, local Reynolds number;
t, $= \dfrac{U t^*}{L}$, nondimensional time;
u, $= u^*/U$, nondimensional velocity in surface direction;
U, reference velocity;
v, $= \left(\dfrac{UL\rho}{\mu}\right)^{1/2} v^*/U$, nondimensional velocity in direction normal to surface;
V, transformed normal velocity, see equation (9c);
x, x^*/L, nondimensional coordinate along surface of wedge;
y, $= \left(\dfrac{UL\rho}{\mu}\right)^{1/2} y^*/L$, nondimensional coordinate normal to wedge.

Greek symbols

β, wedge angle, see equation (2);
ζ, similarity coordinate, see equation (8a);
η, transformed normal coordinate, see equation (8b);
θ, $= \dfrac{T - T_e}{T_w - T_e}$, nondimensional temperature;
μ, fluid viscosity;
ξ, transformed coordinate, see equation (1b);
ρ, fluid density;
σ_s, surface shear stress;
τ, similarity coordinate, see equation (14).

Subscripts

e, conditions at edge of boundary layer;
w, conditions at surface of wedge.

Superscript

*, dimensional quantity.

INTRODUCTION

THE PROBLEM of heat transfer in the laminar boundary layer resulting from the flow of an incompressible fluid past a semi-infinite wedge set impulsively into motion is of considerable practical and theoretical interest. The heat-transfer problem is idealized as follows. The wedge and the fluid are assumed to be initially at the same temperature. A forced-convection thermal boundary layer is then produced by the sudden imposition of a constant temperature difference between the wedge and the fluid as the motion is started. The simultaneous development of the thermal and momentum boundary layers is the subject to be considered herein.

The evolution of the boundary-layer flow in time is characterized by the existence of three distinct flow regions. Initially, at a fixed position along the surface of the wedge the boundary layers formed are independent of upstream flow history. For a flat plate this region is equivalent to the flow analyzed by Rayleigh [1] for an infinite plate. Ultimately, the flow tends to the familiar self-similar, steady, Falkner–Skan or Blasius momentum boundary layers with their associated thermal boundary layers. The intermediate region in which the flow develops from the initial to the ultimate state is somewhat more complex and its solution is more difficult to obtain.

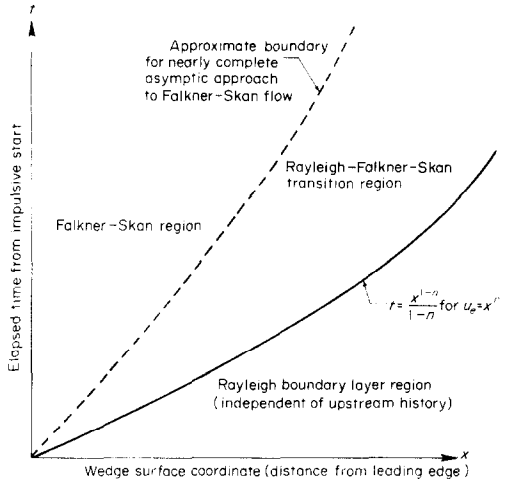

FIG. 1. Viscous flow regions for impulsive wedge flow.

A unified approach to the solution of the boundary-layer equations in the three regions is presented in this paper. The characteristic arrangement of these regions in the x–t plane is illustrated in Fig. 1.

The salient features of the formulation of the problem were described by Stewartson [2] and an approximate solution obtained for the momentum boundary layer over a flat plate. Approximate solutions of various kinds for the flat plate problem have also been obtained by several subsequent investigators including Schuh [3], Oudart [4], and Cheng and Elliot [5]. These approximate solutions suffer from a lack of detail. The later numerical solutions of Dwyer [6], Hall [7] and Dennis [8] are significant improvements on the earlier approximate techniques. Yalamanchili and Benzkofer [9] discuss the solution of the problem by the method of weighted residuals with the method of lines. More recently, Watkins [10] describes the numerical solution by Hall's [7] method of the associated thermal boundary layer for the flat plate.

An approximate solution of the momentum boundary layer for the more general impulsive wedge flow problem was obtained by Smith [11]. This problem was subsequently solved numerically by Nanbu [12] using Hall's basic method with some improved aspects. However, until the present work, no solutions of the thermal boundary layer associated with the Rayleigh–Falkner–Skan momentum boundary layer for wedge flow have appeared in the literature.

ANALYSIS

Impulsive flow

The dimensionless velocity for inviscid potential flow over a sharp wedge is given by

$$u_e = x^n, \quad n \leqslant 1 \tag{1}$$

where x is the dimensionless distance along the surface from the leading edge. The exponent n is related to the wedge angle $\pi\beta$ where

$$\beta = \frac{2n}{n+1}. \tag{2}$$

In impulsive motion of a wedge in an incompressible fluid, the inviscid flow described by equation (1) is established instantaneously. At the same time, a viscous boundary layer begins to develop adjacent to the surface. However, the boundary-layer approximation dictates that the upstream dependence of the viscous flow propagates with a maximum velocity given by the local inviscid velocity. Therefore, within the boundary layer at a fixed distance x, Rayleigh flow exists until the arrival of the portion of the boundary-layer flow containing upstream history. The arrival time is

$$t = \int_0^x \frac{\mathrm{d}\chi}{u_e(\chi)}. \tag{3}$$

From which for $n \neq 1$

$$t = \frac{x^{1-n}}{(1-n)}. \tag{4}$$

For $n = 1$, the stagnation boundary layer, t becomes infinite and the boundary layer remains Rayleigh in character.

General equations

Sufficiently far downstream of the leading edge, the governing equations are the unsteady Prandtl boundary-layer equations for impulsive flow. In nondimensional form these equations are:

$$\frac{\partial u}{\partial x} + \frac{\partial v}{\partial y} = 0 \tag{5a}$$

$$\frac{\partial u}{\partial t} + u\frac{\partial u}{\partial x} + v\frac{\partial u}{\partial y} = u_e\frac{\partial u_e}{\partial x} + \frac{\partial^2 u}{\partial y^2} \tag{5b}$$

$$\frac{\partial T}{\partial t} + u\frac{\partial T}{\partial x} + v\frac{\partial T}{\partial y} = \frac{1}{Pr}\frac{\partial^2 T}{\partial y^2} \tag{5c}$$

where the effects of frictional heat have been neglected. The boundary conditions on equations (5) are, at the surface of the plate

$$y = 0 \quad \begin{matrix} u = v = 0 & \text{for any } t \\ T = T_w & \text{for } t \geqslant 0. \end{matrix} \tag{6}$$

At the boundary layer edge

$$y \to \infty \quad \begin{matrix} u = u_e(x) & t \geqslant 0 \\ T = T_e & \text{for any } t. \end{matrix} \tag{7}$$

Similarity

The number of independent variables in the governing equations can be reduced from three to two by transforming equations (5) into similarity form. This is accomplished by introducing the new independent variables

$$\zeta = \frac{x^{1-n}}{(1-n)t} \tag{8a}$$

$$\eta = \left(\frac{1+n}{2}\right)^{1/2} x^{(n-1)/2} y \tag{8b}$$

such that $\zeta = 1$ represents the boundary between the Rayleigh and Falkner–Skan region. Rayleigh flow exists for $\zeta \geqslant 1$.

New dependent variables are defined as follows:

$$f' = u/u_e \qquad \theta = \frac{T-T_e}{T_w-T_e} \tag{9a,b}$$

$$V = vy/\eta - f'\delta\eta \tag{9c}$$

where

$$\delta = \frac{1-n}{1+n}.$$

The transformed equations are:

$$\frac{\partial V}{\partial \eta} + 2\delta\zeta\frac{\partial f'}{\partial \zeta} + f' = 0 \tag{10a}$$

$$2\delta\zeta(f'-\zeta)\frac{\partial f'}{\partial \zeta} + \beta(f'^2-1) + V\frac{\partial f'}{\partial \eta} - \frac{\partial^2 f'}{\partial \eta^2} = 0 \tag{10b}$$

$$2\delta\zeta(f'-\zeta)\frac{\partial \theta}{\partial \zeta} + V\frac{\partial \theta}{\partial \eta} - \frac{1}{Pr}\frac{\partial^2\theta}{\partial \eta^2} = 0. \tag{10c}$$

The transformed boundary conditions are, at the surface

$$\eta = 0 \qquad \begin{matrix} f' = V = 0 \\ \theta = 1. \end{matrix} \tag{11}$$

At the boundary-layer edge

$$\eta \to \infty \qquad \begin{matrix} f' = 1 \\ \theta = 0. \end{matrix} \tag{12}$$

Equations (10) are singular for the case $n = 1$ (stagnation flow) with this particular choice of similarity variables. The case $n = 1$ will be treated separately. It should be noted that as $\zeta \to 0$ the ordinary differential equations for fully-developed Falkner–Skan boundary-layer flow are recovered. These are:

$$\frac{\partial V}{\partial \eta} + f' = 0 \tag{13a}$$

$$\beta(f'^2-1) + V\frac{\partial f'}{\partial \eta} - \frac{\partial^2 f'}{\partial \eta^2} = 0 \tag{13b}$$

$$V\frac{\partial \theta}{\partial \eta} - \frac{1}{Pr}\frac{\partial^2\theta}{\partial \eta^2} = 0. \tag{13c}$$

Nonsingular Rayleigh flow equations

The singularity in equations (10) for the case $n = 1$ can be removed by a change of independent variable. The relationship between the new independent variable τ and the old independent variable ζ is given by

$$\tau = \frac{1}{\delta\zeta} = t(n+1)x^{n-1}. \tag{14}$$

Equations (10) then become

$$\frac{\partial V}{\partial \eta} - 2\tau\delta\frac{\partial f'}{\partial \tau} + f' = 0 \tag{15a}$$

$$(2-2\tau\delta f')\frac{\partial f'}{\partial \tau} + \beta(f'^2-1) + V\frac{\partial f'}{\partial \eta} - \frac{\partial^2 f'}{\partial \eta^2} = 0 \tag{15b}$$

$$(2-2\tau\delta f')\frac{\partial \theta}{\partial \tau} + V\frac{\partial \theta}{\partial \eta} - \frac{1}{Pr}\frac{\partial^2\theta}{\partial \eta^2} = 0. \tag{15c}$$

This form is also convenient in the numerical integration procedure used in the Rayleigh region $(0 < \tau < 1/\delta)$ for all cases, including $n = 1$. The procedure will be described in a later section.

NUMERICAL SOLUTION TECHNIQUES

Fundamental approach

Equations (10) resemble the equations for steady two-dimensional nonsimilar boundary layers. Unfortunately, in this case the equations cannot be solved by the well-known step-by-step initial value methods normally used for the numerical solution of two-dimensional boundary layers [13], due to the presence of the apparent convective velocity term $(f'-\zeta)$. The term will be negative in regions of the flow where $f' < \zeta$, simulating a reverse-flow boundary layer with its attendant solution difficulties. Such difficulties are caused by the necessity of including the effects of downstream influences in regions of the boundary layer where the flow is locally reversed [14]. Because of this requirement, the problem in the transformed domain must be posed as a boundary-value problem. The boundary values at the upstream end ($\zeta = 0$) are given by the Falkner–Skan equations, equations (13). At the downstream end the situation is less obvious. However, if the downstream boundary is taken as some point within the Rayleigh region ($\zeta \geqslant 1$), boundary values that are independent of the flow in the transition region can be obtained by separate solution of the Rayleigh region. For the flat plate the boundary layer equations in the Rayleigh region simplify to a form having an exact solution [10]. This simplification does not apply to the wedge so that a more general approach must be taken. Since in the Rayleigh flow region $(f'-\zeta)$ is always negative, the solution of equations (10) for Rayleigh flow can be accomplished by the step-by-step integration of equations (10) starting at some point sufficiently far downstream for the initial condition to be approximated, and then marching upstream until the boundary is reached.

It is advantageous to perform this integration in terms of the independent variable τ over the finite range $0 \leqslant \tau \leqslant \tau_1$, where $\tau_1 < 1/\delta$, with the equations in the form given by equations (15).

The previous approaches to the numerical solution of this problem are basically of two types. The first, due to Hall [6], is to attack the nonsimilar equations directly with a time-dependent numerical method using an iterative procedure based on satisfying the similarity condition to obtain a starting approximation. The second appraoch [7] is to finite difference the equations in similarity variables solving the problem iteratively in the transition region as a boundary value problem. First-order upwind differencing is used for the convective terms in the reverse flow.

The approach used in the present work is relatively simple conceptually and is a satisfactory alternative to the aforementioned approaches. It is akin to the method used for the solution of a quasi-steady boundary layer with an oscillatory free stream by Phillips and Ackerberg [15]. In applying the present method, the problem

is formulated as a time-dependent problem in transformed coordinates whose asymptotic steady solution for large time is the solution to the similar equations, equations (10). A second-order finite-difference method for three-dimensional and unsteady boundary layers with reverse flow is used to obtain the time-asymptotic solution. This procedure, while exploiting the self-similar nature of the solution, allows the computation of more complex impulsively started boundary layers through the retention of explicit time-dependence. For example, the method can be easily extended to compute the oscillatory boundary layer or to compute the case where there is a nonuniform free convection thermal boundary layer existing before the impulsive start.

Transition region

The governing equations can be written retaining their explicit time-dependence in terms of modified similarity variables, with a new independent variable ξ defined as

$$\xi = \frac{x^{1-n}}{(1-n)(t+b)}, \quad b > 0 \tag{16}$$

where b is a constant.

Equations (5) become

$$\frac{\partial V}{\partial \eta} + 2\delta\xi\frac{\partial f'}{\partial \xi} + f' = 0 \tag{17a}$$

$$2\delta(t+b)\xi\frac{\partial f'}{\partial t} + 2\delta\xi(f'-\xi)\frac{\partial f'}{\partial \xi} + \beta(f'^2-1) + V\frac{\partial f'}{\partial \eta} - \frac{\partial^2 f'}{\partial \eta^2} = 0 \tag{17b}$$

$$2\delta(t+b)\xi\frac{\partial \theta}{\partial t} + 2\delta\xi(f'-\xi)\frac{\partial \theta}{\partial \xi} + V\frac{\partial \theta}{\partial \eta} - \frac{1}{Pr}\frac{\partial^2 \theta}{\partial \eta^2} = 0. \tag{17c}$$

The surface and inviscid flow boundary conditions for equations (17) are given by equations (11) and (12). A positive nonzero requirement is placed on the constant b such that equations (17) initially apply to a region of the wedge $0 < x \leqslant x_0$, finite in extent.

This condition is necessary for the stability of the difference scheme as will be discussed later. It also allows the simultaneous integration of the equations for the Rayleigh flow region with the integration of equations (17). The constant b is related to the initial extent of the region such that for $t = 0$ at $\xi = 1$

$$x = x_0 = [b(1-n)]^{1/(1-n)}. \tag{18}$$

For sufficiently large times, the solution of equations (17) must asymptotically approach the solution of equations (10).

Rayleigh region

The Rayleigh flow solution of equations (15) serves as the downstream end boundary condition for the numerical solution of equations (17). In the present work this boundary condition is applied at $\xi = 1{\cdot}25$. For $\xi = 1{\cdot}25$ from equations (16) and (14) there is a correspondence between τ ant t expressed by the relation

$$\tau = \tau_1 \frac{t}{t+b} \tag{19}$$

where $\tau_1 = 0{\cdot}8/\delta$.

Therefore, the time-dependent downstream boundary condition for equations (17) can be obtained from the numerical integration of equations (15) advancing τ according to equation (19) as time is advanced from $t = 0$ to the asymptotic limit. The choice of $\xi = 1{\cdot}25$ for the downstream boundary which yielded $\tau_1 = 0{\cdot}8/\delta$ was made from experience; the step-by-step numerical integration of equations (15) becomes difficult for τ significantly larger than $0{\cdot}8/\delta$. A smooth initial profile for the solution of equations (15) is desirable to avoid problems in starting the numerical integration. It can be obtained from the leading term in the perturbation solution for small τ [16] of each of equations (15a) and (15b)

$$f' = \operatorname{erf}[\eta/\sqrt{(2\tau)}] + \ldots \tag{20a}$$

$$\theta = \operatorname{erfc}[\eta/\sqrt{(2\tau/Pr)}] + \ldots. \tag{20b}$$

The surface and inviscid flow boundary conditions for equations (15) applicable for all τ are given by equations (11) and (12).

Upstream boundary and initial conditions

With the Rayleigh flow as the downstream boundary, the other imposed end boundary condition for the numerical solution of equations (17) is the solution of the Falkner–Skan equations, equations (13), since equations (17) reduce to the Falkner–Skan equations at the upstream ($\xi = 0$) boundary. The surface and inviscid flow boundary conditions are given by equations (11) and (12).

The appropriate initial conditions for the solution of the time-dependent equations, equations (17) are at $t = 0$ for $\eta > 0$ and $0 < \xi < 1{\cdot}25$

$$f' = 1; \qquad \theta = 0. \tag{21}$$

Figure 2 illustrates schematically the solution procedure in the $\xi - t$ plane.

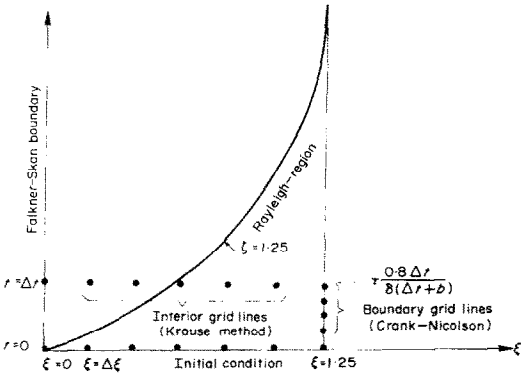

FIG. 2. Computational scheme.

Finite difference methods

The Krause second-order, zig-zag, finite-difference scheme [17] was used for the time-dependent numerical solution of equations (17). It has the feature of utilizing downstream information at an earlier time in the development of the flow as well as current upstream information to predict the properties of a boundary layer containing local flow reversal.

The method was developed for and has been successfully applied to steady three-dimensional boundary layers with flow reversal [18], [19]. The unsteady boundary layer can be regarded as a special case of the three-dimensional boundary layer with one surface direction viewed as a time-like coordinate. The procedures for the numerical solution are virtually identical.

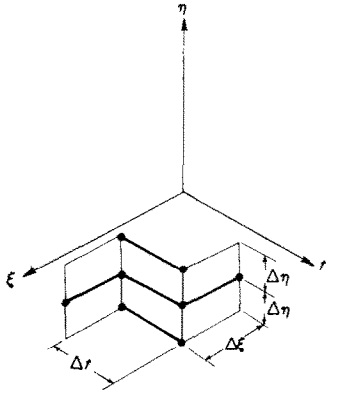

FIG. 3. Computational molecule for Krause method.

In the present calculation, the computational molecule for the method was oriented as shown in Fig. 3. Details of the derivation of finite-difference equations for the application of the Krause method are given in [18] and [19]. The method is an implicit technique.

For stability [17] and to avoid the amplification of round-off errors [20] the time step limitation for the Krause method is

$$\Delta t \leqslant \frac{\Delta\xi(t+b)}{|f'-\xi|_{\max}} \tag{22}$$

which for the present computation effecitvely requires

$$\Delta t \leqslant \Delta\xi(t+b). \tag{23}$$

Hence, at $t = 0$ difficulties are avoided by requiring $b > 0$. The magnitude of b can also be utilized as a parameter to adjust the relative amounts of upstream and previous-time information used in the approach to the asymptotic steady state. In the present work a value of b was used corresponding to $x_0 = 2{\cdot}0$.

The step-by-step solution of equations (15) at the downstream boundary was obtained using the Crank–Nicolson finite-difference method. The two-point boundary value problem posed by the Falkner–Skan equations at the upstream boundary was solved using the finite-difference method described in [21].

RESULTS AND DISCUSSION

Solutions were computed for $n = 1{\cdot}0$, $0{\cdot}3333$, $0{\cdot}1111$, $0{\cdot}0$, $-0{\cdot}0654$, and $-0{\cdot}0905$, corresponding to wedge angles of π, $\pi/2$, $\pi/5$, 0, $-0{\cdot}14\pi$ and, $-0{\cdot}199\pi$ respectively. Results were obtained for several different Prandtl numbers in the intermediate range from $Pr = 0{\cdot}7$ to $Pr = 10{\cdot}0$.

In the time-asymptotic calculation for the transition region the mesh (grid) interval $\Delta\tau$ was taken as $0{\cdot}05$. The time-step Δt was $0{\cdot}99$ of the maximum permissible given by equation (23). Steady-state convergence was achieved after approximately 200 time-steps. In the Rayleigh region the maximum integration step size $\Delta\tau$ was $0{\cdot}005$. As many as 180 mesh intervals were used in the calculation normal to the surface. To reduce the amount of computer time required in the transition region calculation, the mesh was rezoned in the normal direction from a lesser number of mesh intervals as the steady state was approached.

The surface heat transfer results expressed in terms of Nusselt number are summarized for the positive wedge cases in Figs. 4–7. These figures show the variation in the quantity $Nu_x Re_x^{-1/2}$ with the independent variable τ, where $Nu_x Re_x^{-1/2}$ is obtained from the slope of the nondimensional temperature profile through the relation

$$Nu_x Re_x^{-1/2} = -\left(\frac{1+n}{2}\right)^{1/2} \left.\frac{\partial\theta}{\partial\eta}\right|_{\eta=0}. \tag{24}$$

Figures 4–7 can be used to determine the heat-transfer coefficient as a function of time at a given position along the surface of the wedge.

The agreement of the computed heat-transfer results in the asymptotic limit as $\tau \to \infty$ with previously obtained steady-state results [22] is within three significant figures. For reference purposes the temperature profiles and their wall derivatives are presented in tabular form in Tables 1–3 for $Pr = 0{\cdot}7$ and $n = 1{\cdot}0$, $n = 0{\cdot}3333$ and $n = 0{\cdot}0$.

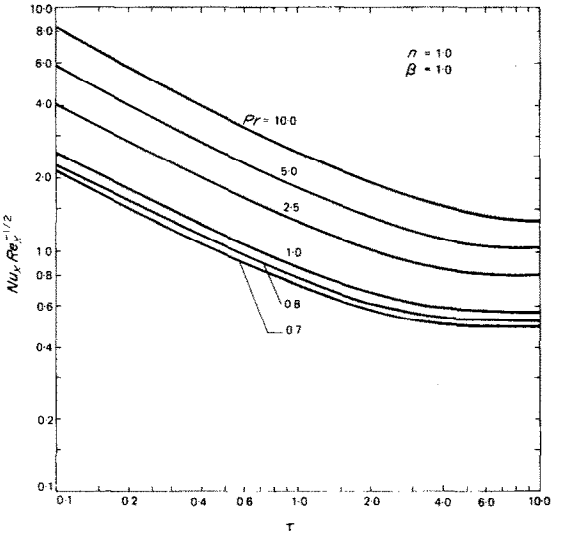

FIG. 4. Nusselt number variation for $n = 1{\cdot}0$.

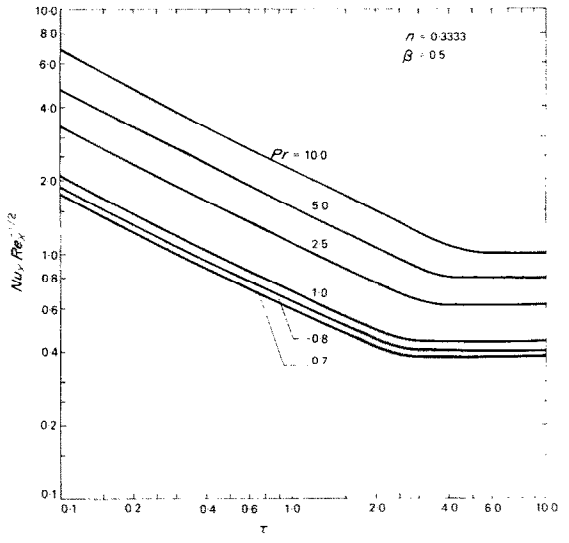

FIG. 5. Nusselt number variation for $n = 0{\cdot}3333$.

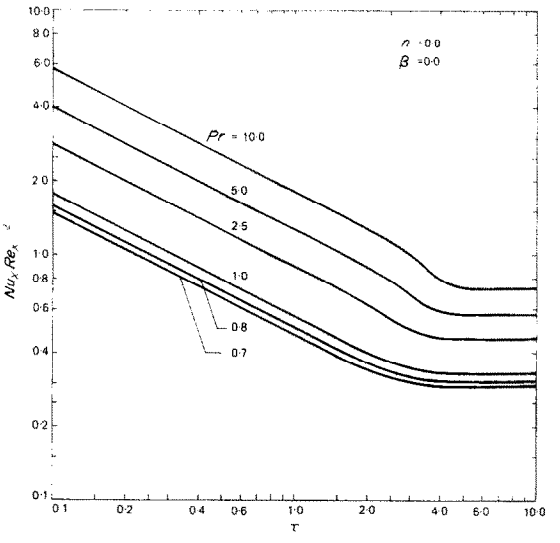

FIG. 7. Nusselt number variation for $n = 0{\cdot}0$.

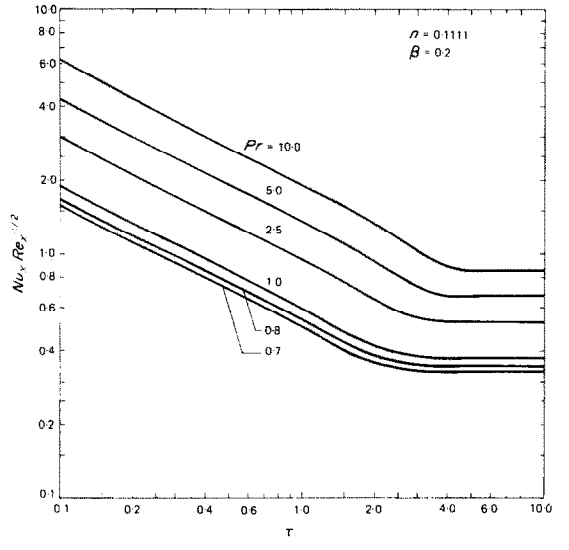

FIG. 6. Nusselt number variation for $n = 0{\cdot}1111$.

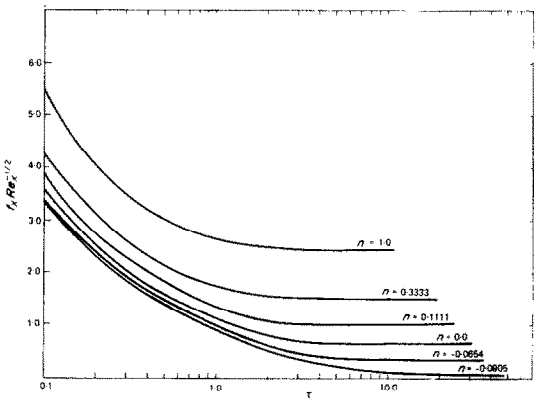

FIG. 8. Friction coefficient variation.

Figure 8 shows the computed variation of surface shear stress in terms of the friction coefficient f_x, where $f_x Re_x^{1/2}$ is obtained from the slope of the nondimensional velocity profiles through the relation

$$f_x Re_x^{1/2} = [2(1+n)]^{1/2} \left.\frac{\partial f'}{\partial \eta}\right|_{\eta=0}. \tag{25}$$

Figure 8 includes the friction coefficient for the two negative wedge angle cases computed, one of them being the incipient separation case of $n = -0{\cdot}0905$. The heat-transfer solutions for the negative cases were not computed because of the contrived nature of the physical flow situation that these cases represent (suction preceeding a turn). The present results given in Fig. 8, agree closely with previously published results for the momentum boundary layers on flat plates and wedges given in [6], [7] and [11].

Table 4 compares the present shear stress results for $n = 0$ with the results of previous investigations. Because of the difference between the computational mesh used in the present calculation and that used by Nanbu [11], no direct comparison is possible in the results for $n \neq 0$. However, by interpolating between mesh points for these cases, the agreement in results appears to be typified by the reasonably close agreement of Table 4. Greater accuracy than that of the present results can be achieved by refining the grid. This would, of course, increase the computer time required. Since in the present investigation many cases were computed, it was felt that three significant figures was sufficient accuracy for the heat-transfer results obtained. Each combination thermal/momentum boundary layer case consumed approximately 10–18 min IBM 370/145 CPU time, depending on the Prandtl number. Calculations for the larger Prandtl number cases utilized a finer grid and consequently, more time.

In conclusion, the present work indicates that the time–asymptotic finite-difference technique can be used to advantage in the computation of the unsteady laminar momentum and thermal boundary layers for Rayleigh–Falkner–Skan flows. Further, the results obtained can be used to estimate the transient heat transfer to wedge shapes undergoing unsteady motion characterized by rapid acceleration to a constant velocity.

Table 1. Values of the complimentary nondimensional temperature $1-\theta$ as a function of η and τ for $n = 1{\cdot}0$ and $Pr = 0{\cdot}7$

η	$\tau =$ $-\partial\theta/\partial\eta =$	0·1 2·14	0·5 0·989	1·0 0·729	2·0 0·582	4·0 0·510	10·0 0·496	∞ 0·496
0·0		0·0000	0·0000	0·0000	0·0000	0·0000	0·0000	0·0000
0·1		0·2107	0·0987	0·0736	0·0582	0·0510	0·0496	0·0496
0·2		0·4072	0·1961	0·1467	0·1162	0·1020	0·0992	0·0992
0·3		0·5780	0·2909	0·2189	0·1739	0·1528	0·1487	0·1487
0·4		0·7162	0·3818	0·2897	0·2311	0·2035	0·1980	0·1980
0·5		0·8200	0·4676	0·3584	0·2874	0·2537	0·2470	0·2470
0·6		0·8927	0·5473	0·4247	0·3428	0·3034	0·2955	0·2955
0·7		0·9398	0·6202	0·4880	0·3968	0·3523	0·3435	0·3435
0·8		0·9684	0·6856	0·5479	0·4492	0·4003	0·3906	0·3906
0·9		0·9844	0·7434	0·6040	0·4997	0·4472	0·4367	0·4367
1·0		0·9928	0·7936	0·6560	0·5481	0·4926	0·4815	0·4815
1·2		0·9987	0·8722	0·7469	0·6376	0·5786	0·5668	0·5668
1·4		0·9998	0·9254	0·8203	0·7162	0·6569	0·6450	0·6450
1·6		1·0000	0·9590	0·8769	0·7833	0·7264	0·7149	0·7149
1·8		1·0000	0·9787	0·9188	0·8387	0·7865	0·7759	0·7759
2·0		—	0·9896	0·9483	0·8830	0·8370	0·8277	0·8277
2·5		—	0·9984	0·9980	0·9532	0·9247	0·9193	0·9193
3·0		—	0·9995	0·9994	0·9838	0·9697	0·9675	0·9675
4·0		—	0·9999	0·9996	0·9982	0·9974	0·9968	0·9968
5·0		—	1·0000	0·9999	0·9999	0·9999	0·9999	0·9999
6·0		—	—	1·0000	1·0000	1·0000	1·0000	1·0000

Table 2. Values of the complimentary nondimensional temperature $1-\theta$ as a function of η and τ for $n = 0{\cdot}3333$ and $Pr = 0{\cdot}7$

η	$\tau =$ $\zeta =$ $-\partial\theta/\partial\eta =$	0·1 20·0 2·13	0·5 4·0 0·961	1·60 1·25 0·552	2·0 1·0 0·508	4·0 0·5 0·471	10·0 0·2 0·471	∞ 0·0 0·471
0·0		0·0000	0·0000	0·0000	0·0000	0·0000	0·0000	0·0000
0·1		0·2098	0·0958	0·05512	0·0508	0·0471	0·0471	0·0471
0·2		0·4054	0·1903	0·1100	0·1015	0·0941	0·0941	0·0941
0·3		0·5755	0·2822	0·1645	0·1519	0·1411	0·1411	0·1411
0·4		0·7132	0·3702	0·2183	0·2020	0·1879	0·1879	0·1879
0·5		0·8171	0·4535	0·2713	0·2515	0·2346	0·2345	0·2345
0·6		0·8901	0·5310	0·3231	0·3003	0·2809	0·2808	0·2808
0·7		0·9379	0·6021	0·3737	0·3482	0·3267	0·3266	0·3266
0·8		0·9670	0·6665	0·4229	0·3951	0·3718	0·3718	0·3718
0·9		0·9835	0·7239	0·4704	0·4407	0·4162	0·4162	0·4162
1·0		0·9923	0·7743	0·5160	0·4851	0·4596	0·4596	0·4596
1·2		0·9985	0·8549	0·6013	0·5690	0·5428	0·5428	0·5428
1·4		0·9997	0·9116	0·6777	0·6456	0·6201	0·6201	0·6201
1·6		0·9999	0·9489	0·7447	0·7142	0·6904	0·6904	0·6903
1·8		1·0000	0·9721	0·8019	0·7742	0·7527	0·7527	0·7526
2·0		1·0000	0·9854	0·8497	0·8253	0·8067	0·8067	0·8065
2·5		—	0·9975	0·9318	0·9166	0·9053	0·9053	0·9052
3·0		—	0·9993	0·9733	0·9659	0·9600	0·9600	0·9599
4·0		—	1·0000	0·9974	0·9964	0·9957	0·9957	0·9955
5·0		—	—	1·0000	1·0000	1·0000	1·0000	0·9999
6·0		—	—	—	—	—	—	1·0000

Table 3. Values of the complimentary nondimensional temperature $1-\theta$ as a function of η and τ for $n = 0{\cdot}0$ and $Pr = 0{\cdot}7$

	$\tau =$	1·0	0·5	0·8	1·0	2·0	5·0	∞
	$\zeta =$	10·0	2·0	1·25	1·0	0·5	0·2	0·0
η	$-\partial\theta/\partial\eta =$	2·12	0·946	0·746	0·668	0·487	0·414	0·414
0·0		0·0000	0·0000	0·0000	0·0000	0·0000	0·0000	0·0000
0·1		0·2088	0·0944	0·0889	0·0661	0·0486	0·0414	0·0414
0·2		0·4036	0·1874	0·1764	0·1317	0·9708	0·0828	0·0828
0·3		0·5730	0·2780	0·2617	0·1964	0·1453	0·1242	0·1242
0·4		0·7104	0·3649	0·3436	0·2598	0·1931	0·1656	0·1655
0·5		0·8143	0·4470	0·4214	0·3214	0·2404	0·2068	0·2067
0·6		0·8877	0·5237	0·4940	0·3809	0·2870	0·2478	0·2477
0·7		0·9360	0·5942	0·5613	0·4380	0·3327	0·2886	0·2885
0·8		0·9656	0·6581	0·6230	0·4925	0·3775	0·3291	0·3290
0·9		0·9826	0·7152	0·6788	0·5440	0·4213	0·3691	0·3690
1·0		0·9917	0·7655	0·7288	0·5925	0·4637	0·4086	0·4085
1·2		0·9984	0·8465	0·8119	0·6797	0·5445	0·4856	0·4855
1·4		0·9997	0·9041	0·8744	0·7537	0·6191	0·5591	0·5590
1·6		0·9999	0·9428	0·9193	0·8149	0·6867	0·6280	0·6279
1·8		1·0000	0·9674	0·9503	0·8641	0·7468	0·6916	0·6915
2·0		—	0·9822	0·9707	0·9025	0·7991	0·7490	0·7489
2·5		—	0·9965	0·9936	0·9619	0·8971	0·8626	0·8626
3·0		—	0·9991	0·9989	0·9872	0·9541	0·9345	0·9345
4·0		—	1·0000	0·9999	0·9991	0·9942	0·9906	0·9906
5·0		—	—	1·0000	1·0000	0·9997	0·9994	0·9993
6·0		—	—	—	—	1·0000	0·1000	1·0000

Table 4. Comparison of present surface shear results $f_x Re_x^{1/2}$ with previous solutions

τ	Present calculation	Hall [7]	Dennis [8]	Nanbu [12]	Rayleigh [1]	Blasius
0·1	3·5860	—	—	—	3·5682	—
0·5	1·6006	—	—	1·5967	1·5967	—
1·0	1·1245	1·1284	1·1284	1·1284	1·1284	—
2·0	0·8047	0·8050	0·8052	—	—	—
4·0	0·6693	0·6690	0·6694	—	—	—
∞	0·6642	0·6640	0·6642	—	—	0·6642

Acknowledgement—This work was supported by National Science Foundation Grant No. GY-11056.

REFERENCES

1. Lord Rayleigh, On the motion of solid bodies through viscous liquids, *Phil. Mag.* **21**, 697–711 (1911).
2. K. Stewartson, On the impulsive motion of a flat plate in a viscous fluid, *Q. Jl Mech. Appl. Math.* **4**, 182–198 (1951).
3. H. Schuh, Calculations of unsteady boundary layers in two-dimensional laminar flow, *Z. Flugwiss.* **1**, 122–131 (1953).
4. A. Oudart, Mise en regime de la couche limite de la plaque plane dans l'impulsion brusque a partir du repos, *Recherche Aeronaut.* **31**, 7–12 (1953).
5. S.-I. Cheng and D. Elliot, The unsteady laminar boundary layer on a flat plate, *Trans. Am. Soc. Mech. Engrs* **79**, 725–733 (1957).
6. H. A. Dwyer, Calculation of unsteady leading edge boundary layers, *AIAA Jl* **6**, 2447–2448 (1968).
7. M. G. Hall, The boundary layer over an impulsively started flat plate, *Proc. R. Soc.* **310A**, 401–414 (1969).
8. S. C. R. Dennis, The motion of a viscous fluid past an impulsively started semi-infinite flat plate, *J. Inst. Math. Appl.* **10**, 105–117 (1972).
9. R. V. S. Yalamanchili and P. D. Benzkofer, Unsteady compressible boundary layers with arbitrary pressure gradients, AIAA paper 73-132 (1973).
10. C. B. Watkins, Heat transfer in the boundary layer over an impulsively started flat plate, *J. Heat Transfer* **97**, 482–484 (1975).
11. S. H. Smith, The impulsive motion of a wedge in a viscous fluid, *Z. Angew. Math. Phys.* **18**, 508 (1967).
12. B. K. Nanbu, Unsteady Falkner–Skan flow, *Z. Angew. Math. Phys.* **22**, 1167–1172 (1971).
13. F. G. Blottner, Finite difference methods of solution of the boundary-layer equations, *AIAA Jl* **8**, 193–205 (1970).
14. J. B. Klemp and A. Acrivos, A method of integrating the boundary-layer equations through a region of reverse flow, *J. Fluid Mech.* **53**, 177–191 (1972).
15. J. H. Phillips and R. C. Ackerberg, A numerical method for integrating the unsteady boundary-layer equations when there are regions of backflow, *J. Fluid Mech.* **58**, 561–579 (1973).
16. H. Schlicting, *Boundary Layer Theory*. McGraw-Hill, New York (1968).
17. E. H. Krause and T. Bothmann, Numerische Stabilitat

Dreidimensionaler, Grenzschictlosungen, *Z. Angew. Math. Mech.* **48**, 1336–1342 (1968).
18. F. G. Blottner, and M. A. Ellis, Finite difference solution of the incompressible three-dimensional boundary layer equations for a blunt body, *Computers & Fluids* **1**, 133–158 (1973).
19. C. B. Watkins, Numerical solution of the three-dimensional boundary layer on a spinning sharp body at angle of attack, *Computers & Fluids* **1**, 317–329 (1973).
20. K. V. Roberts and N. O. Weiss, Convective difference schemes, *Math. Comp.* **20**, 279–298 (1966).
21. C. B. Watkins and F. G. Blottner, Three-dimensional effects on electron density in a blunt body laminar boundary layer, *AIAA Jl* **10**, 1332–1338 (1972).
22. H. L. Evans, Mass transfer through laminar boundary layers—7. Further similar solutions to the *b*-equation for the case $B = 0$, *Int. J. Heat Mass Transfer* **5**, 35–57 (1962).

TRANSFERT DE CHALEUR INSTATIONNAIRE DANS LES ECOULEMENTS IMPULSIFS DE FALKNER–SKAN

Résumé—On présente des solutions numériques du transfert de chaleur dans une couche limite laminaire instationnaire résultant de l'écoulement incompressible sur un coin semi-infini mis brusquement en mouvement. Le mouvement du coin est uniforme après l'impulsion de départ. A l'instant initial du mouvement, une couche limite thermique en convection forcée est produite par l'application brutale d'une différence de température constante entre le coin et le fluide. Les solutions pour le développement simultané des couches limites thermiques et dynamiques ont été obtenues à l'aide d'une méthode de différences finies par une convergence dans le temps. Les résultats des calculs sont présentés pour plusieurs angles du coin et pour des nombre de Prandtl moyens.

INSTATIONARER WARMEUBERGANG IN IMPULS-FALKNER–SKAN-STRÖMUNGEN

Zusammenfassung—Numerische Lösungen werden für den Wärmeübergang beschrieben in einer instationären laminaren Grenzschicht bei inkompressibler Strömung an einem halbunendlichen Keil mit Anfangsimpuls. Die Bewegung des Keils ist nach dem Anfangsimpuls stationär. Bei Bewegungsbeginn wird eine thermische Grenzschicht mit Zwangskonvektion erzeugt durch das plötzliche Aufbringen einer konstanten Temperaturdifferenz zwischen Keil und umgebendem Fluid. Lösungen für die gleichzeitige Ausbildung der thermischen und hydrodynamischen Grenzschicht werden mit Hilfe eines zeitasymptotischen finiten Differenzenverfahrens gewonnen. Die Ergebnisse der Berechnungen werden für verschiedene Keilwinkel angegeben, mit Prandtl–Zahlen in einem mittleren Bereich.

НЕСТАЦИОНАРНЫЙ ТЕПЛООБМЕН В ИМПУЛЬСНО ВОЗБУЖДАЕМЫХ ПОТОКАХ ФОЛКНЕРА–СКЭНА

Аннотация — Приводятся численные решения теплообмена в нестационарном ламинарном пограничном слое, возникающем в несжимаемой жидкости при обтекании внезапно начавшего двигаться полубесконечного клина. После импульсного начала движение стационарно. Тепловой пограничный слой при вынужденной конвекции создается за счет внезапного наложения постоянной разности температур между клином и жидкостью одновременно с началом движения.

С помощью временно-асимптотического конечно-разностного метода получены решения для одновременного развития теплового и динамического пограничных слоёв. Приводятся результаты расчетов для нескольких углов раствора клина в диапазоне промежуточных значений чисел Прандтля.